Available online at www.sciencedirect.com

ScienceDirect

Journal of the Franklin Institute 350 (2013) 2455–2473

Journal of The Franklin Institute

www.elsevier.com/locate/jfranklin

Autonomous impulsive rendezvous for spacecraft under orbital uncertainty and thruster faults

Zhan Li, Xuebo Yang, Huijun Gao*

Research Institute of Intelligent Control and Systems, Harbin Institute of Technology, Harbin 150080, China

Received 31 March 2012; received in revised form 4 July 2012; accepted 5 July 2012
Available online 10 August 2012

Abstract

This paper investigates the reliable impulsive control problem for autonomous spacecraft rendezvous under the orbital uncertainty and possible thruster faults. The orbital uncertainty is described as the model uncertainty, and the possible thruster faults are modelled by scaling factors. By introducing a state-feedback controller, the autonomous rendezvous problem is regarded as an asymptotic stabilization problem of a switching system composed of impulse action phase and free motion phase. Based on Lyapunov theory and genetic algorithms (GA), a reliable impulsive controller design approach is proposed. With the obtained controller, the autonomous spacecraft rendezvous is accomplished by a series of proper impulse thrust in spite of the orbital uncertainty and the possible thruster faults. The effectiveness of the proposed approach is illustrated by simulation examples.

1. Introduction

With the rapid development of astronautic technique during the last few decades, the orbital control problem of autonomous spacecraft rendezvous has attracted considerable attention due to its importance on many modern complicated aerospace missions such as spacecraft intercepting, repairing, docking or formation networking. For instance, the optimal impulsive control method for spacecraft rendezvous is studied in [6,10,15]; adaptive control theory is applied to the rendezvous and docking problem in [14]; an annealing algorithm method for rendezvous orbital control is proposed in [9]; a multi-objective robust orbital control method based on Lyapunov theory is proposed in

*Corresponding author.
E-mail addresses: lznavy@gmail.com (Z. Li), xueboyang@hit.edu.cn (X. Yang), hjgao@hit.edu.cn (H. Gao).

0016-0032/$32.00
http://dx.doi.org/10.1016/j.jfranklin.2012.07.002

[4]; the sampled-data control problem for spacecraft relative position holding is studied in [20]; a guaranteed cost robust control strategy for spacecraft output tracking during the rendezvous process is presented in [21]. Although there have been many results in this field, the rendezvous orbital control problem has not been fully investigated and still remains challenges.

Impulsive thrust is widely adopted in spacecraft control due to the simplicity for applications. Many studies on the correlative problems have been reported, see, for instance, [5,9–11]. In [9,10], the optimal impulse control strategies based on simulated annealing (SA) are proposed; null controllability with vanishing energy (NCVE) property is studied for the impulsive orbital transfer problem in [5]. However, we noticed that, for most of the proposed methods, the impulse thrust needs to be previously designed before the mission starts. Thus, these impulsive control strategies are actually open-loop control methods, which are easily affected by the external unexpected disturbance or other uncertain factors. Compared with the open-loop control method, the closed-loop impulsive control approach determines the needed impulse thrust according to the real-time states, and thus, the affection caused by the unexpected conditions can be reduced effectively. Obviously, the closed-loop control approach has more advantages than the open-loop control approach. However, the closed-loop impulsive control problem has seldom been studied till now, and this motivates our work in this paper.

The most widely adopted model of relative motion between two adjacent spacecraft is built based on the famous C–W equations, which is derived by Clohessey and Wiltshire in 1960 [1]. For this kind of models, the target orbit is assumed to be circle and the target angular velocity is a constant, which is one of the important parameters of the model. However, the circle orbit is hard to maintain and it is impossible to determine the accurate target angular velocity due to the complex orbital uncertainty caused by external disturbance, equipment errors, mass variation, etc. Thus, guaranteeing robustness for the orbital uncertainty is a big challenge for studies on spacecraft rendezvous problems. In recent years, many kinds of uncertainties existing in many different systems are widely studied [2,12,13,24]. Some efficient approaches towards different kinds of uncertainties have been reported, see, for instance, [3,7,8]. Nevertheless, for the spacecraft rendezvous problem, the orbital uncertainty is always studied separately, and it is necessary to take the design requirements into consideration simultaneously.

As mentioned before, autonomous spacecraft rendezvous is an extremely complicated process with many unexpected factors. Besides the external affections caused by orbital uncertainty we just discussed above, another important issue we cannot ignored is the possible internal problems of the spacecraft, which always happens in the thrusters. Due to the limitation of the technique and the shocking space conditions, it is impossible to completely avoid the thruster faults. Thus, in order to ensure the safety and the accuracy of the rendezvous, the orbital controller with reliability against the possible thruster faults is also significant for the studies on orbital control of autonomous spacecraft rendezvous. Recently, many results of reliable control have been reported. For linear systems, [16,17] present reliable controller design methods which can stabilize the systems and ensure the performances in spite of some admissible control component outages; the reliable control problem for network with random packet losses or missing measurements is studied in [18,19]; a pre-compensator is utilized for a kind of systems with actuator redundancies in [25]. Nevertheless, few results of reliable control problem have been successfully adopted in spacecraft rendezvous process. In [22], the reliable autonomous rendezvous problem is studied based on a model with scaling fault factors. However, the analysis and the results in [22] are all based on the continuous thrust control method. Therefore, it is still a challenge to study the reliable impulsive control problem for spacecraft autonomous rendezvous.

In this paper, the orbital uncertainty and the possible thruster faults are considered synthetically for the impulsive autonomous spacecraft rendezvous problem. By introducing a state-feedback controller, the relative motion system during the impulse action and the free motion phase are regarded as closed-loop system and open-loop system respectively, and the whole rendezvous process is regarded as a switching system composed of these two phases. Then, based on the Lyapunov theory, the autonomous rendezvous problem is regarded as an asymptotic stabilization problem of the switching system. The proper state-feedback controller is obtained by solving a feasibility problem of a set of linear matrix inequalities (LMIs), some of whose proper parameters are previously searched by genetic algorithms (GA). The approach based on GA and LMIs we adopt here has been proven effective for solving the relative orbital transfer problem during the spacecraft rendezvous process, see, for instance, [23]. However, we noticed that, only the basic impulse control problem without consideration of orbital uncertainty and possible thruster faults is studied in [23]. The results of [23] are expanded in this paper. With the controller designed by the proposed method in this paper, the autonomous spacecraft rendezvous process is accomplished under the orbital uncertainty and the possible thruster faults. Some illustrative examples are provided to show the effectiveness of the proposed method.

Notations: The notation used throughout the paper is fairly standard. The superscript "T" stands for matrix transposition; $\mathbb{R}^n$ denotes the n-dimensional Euclidean space and $\mathbb{R}^{n\times m}$ denotes the set of all $n\times m$ real matrices; $\|\cdot\|$ refers to either the Euclidean vector norm or the induced matrix 2-norm. For a real symmetric matrix W, the notation $W>0$ ($W<0$) is used to denote its positive- (negative-) definiteness. diag$\{\ldots\}$ stands for a block-diagonal matrix. For any matrix S, sym$S\}$ means $S+S^T$. In symmetric block matrices or complex matrix expressions, we use an asterisk ($*$) to represent a term that is induced by symmetry. I and 0 denote the identity matrix and zero matrix with compatible dimensions, respectively. Matrices, if their dimensions are not explicitly stated, are assumed to be compatible for algebraic operations.

2. Problem formulation

In this section, the norm-bounded orbital uncertainties and the impulsive thrust with possible thruster faults are considered, and the relative motion model is established based on the C–W equations. Finally, the reliable impulsive orbital control problem is formulated.

2.1. Relative motion with orbital uncertainty

By assuming circular target's orbit and small distance between two spacecraft, the linearized equations of the relative motion between them can be described as

$$\begin{cases} \ddot{x}-2n\dot{y}-3n^2x=a_x, \\ \ddot{y}+2n\dot{x}=a_y, \\ \ddot{z}+n^2z=a_z, \end{cases} \tag{1}$$

where x and y are the radial component and along-track component of the chaser's position relative to the target respectively, z is the out-plane component which completes the right handed coordinate system, n is the target angular velocity, a_i ($i=x$, y, z) is the ith component of the acceleration input of chaser.

The front two equations in Eq. (1) describe the in-plane motion and the third equation describes the out-plane motion respectively, and the two motions are independent. Obviously, the in-plane motion is more complicated than out-plane motion. In this paper, we focus on the in-plane motion, whose results are also suitable for out-plane motion. By defining the state vector $\mathbf{x}(t)=[x,y,\dot{x},\dot{y}]^T$ and the input vector $\mathbf{u}(t)=[a_x,a_y]^T$, the relative motion equations can be written as the following state space function:

$$\dot{\mathbf{x}}(t)=A\mathbf{x}(t)+B\mathbf{u}(t), \tag{2}$$

where the matrices A and B are obtained according to Eq. (1):

$$A=\begin{bmatrix} 0 & 0 & 1 & 0 \\ 0 & 0 & 0 & 1 \\ 3n^2 & 0 & 0 & 2n \\ 0 & 0 & -2n & 0 \end{bmatrix}, \quad B=\begin{bmatrix} 0 & 0 \\ 0 & 0 \\ 1 & 0 \\ 0 & 1 \end{bmatrix}.$$

Obviously, the rendezvous process can be regarded as the asymptotic stabilization process of the system in Eq. (2), and the main task is to determine the proper control input vector $\mathbf{u}(t)$.

As we mentioned in Section 1, matrix A is obtained based on the assumption of n is constant, which means that the target orbit is circle. However, exact circle orbit is difficult to maintain in practice. Thus, in this paper, we consider the state matrix as an uncertain matrix $\tilde{A}=A+\Delta A$, where the orbital uncertainty is considered as a norm-bounded matrix $\Delta A=DF(t)E$, and Eq. (2) is written as

$$\dot{\mathbf{x}}(t)=\tilde{A}\mathbf{x}(t)+B\mathbf{u}(t). \tag{3}$$

The matrices D and E are the constant matrices with proper dimension, $F(t)$ is an unknown real-time varying matrix with Lebesgue measurable elements bounded by $F^T(t)F(t)\leq I$.

2.2. Impulsive thrust with possible thrust faults

For control input $\mathbf{u}(t)$, two kinds of thrusts, continuous thrust and impulsive thrust, can be adopted during the orbital transfer process. However, it is actually difficult to directly obtain the continuous thrust in practice, and the impulsive thrust has been widely adopted for the practical spacecraft control. Therefore, we focus on the impulse thrust control strategy in this paper.

Different from continuous thrust strategy, the impulse control method is realized by a series of impulsive thrust. As the correlative analysis in [23], the whole rendezvous process can be regarded as a series of alternations between impulse action phase and the sequent free motion phase, which can be regarded as closed-loop system and open-loop system respectively. These two phases can be described by the following equations:

$$\begin{aligned} \text{impulse action}: &\quad \dot{\mathbf{x}}(t)=\tilde{A}\mathbf{x}(t)+B\mathbf{u}(t), \quad t_k<t\leq t_k+\tau \\ \text{free motion}: &\quad \dot{\mathbf{x}}(t)=\tilde{A}\mathbf{x}(t), \quad t_k+\tau<t\leq t_{k+1} \end{aligned} \tag{4}$$

where t_k is the instant of the kth impulse, τ is the duration of each impulse. As is well known, the impulsive thrust is always assumed to be generated immediately at t_k, which means that $\tau=0$. However, non-duration is impossible in practical engineering. Thus, the impulse duration is taken into consideration in our study, and making it as short as possible is one of our objectives in this paper.

For the impulse action phase, we consider state-feedback strategy as

$$\mathbf{u}(t)=K\mathbf{x}(t), \quad t_k<t\leq t_k+\tau, \tag{5}$$

where K is the state-feedback gain matrix which needs to be determined. By considering the possible thruster faults, we introduce two parameters $m_x(t)$ and $m_y(t)$ to represent the possible thruster faults along x-and y-axes respectively. Assume that $m_x(t)$ and $m_y(t)$ satisfy $0\leq m_{li}\leq m_i(t)\leq m_{ui}<\infty$, $(i=x,y)$, where m_{li} and m_{ui} are given real constraints. We can see that, if $m_{li}=m_{ui}=1$, then $m_i(k)=1$, which means that there is no fault in thruster. Reversely, if $m_{li}=m_{ui}=0$, then $m_i(k)=0$, which means that the thrust is completely lost. More generally, $0<m_{li}< m_{ui}$ and $m_i(t)\neq 1$ denote that there exists partial fault in the corresponding thruster. Thus, by introducing a fault matrix $M=\text{diag}\{m_x,m_y\}$, the control vector existing possible thruster faults $\mathbf{u}^f(t)$ can be written as

$$\mathbf{u}^f(t)=MK\mathbf{x}(t), \quad t_k<t\leq t_k+\tau. \tag{6}$$

According to Eqs. (4) and (6), the closed-loop system of the impulse action phase can be obtained, and the whole rendezvous process can be rewritten as

$$\begin{aligned} \text{impulse action}: \quad & \dot{\mathbf{x}}(t)=(\tilde{A}+BMK)\mathbf{x}(t), \quad t_k<t\leq t_k+\tau, \\ \text{free motion}: \quad & \dot{\mathbf{x}}(t)=\tilde{A}\mathbf{x}(t), \quad t_k+\tau<t\leq t_{k+1}. \end{aligned} \tag{7}$$

2.3. Problem of the controller design

According to the analysis above, the problem to be studied in this paper can be formulated as:

For the relative motion between two spacecraft which is described by the switching system in Eq. (7), determine the state-feedback gain matrices K such that the needed impulsive thrust can be determined during the rendezvous process, with that the system is asymptotically stable, which means that the rendezvous of the two spacecraft is accomplished by the obtained impulsive thrust under the orbital uncertainty and the possible thruster faults.

3. Controller design

As discussed above, the autonomous spacecraft rendezvous control problem has been transformed into a stabilization problem of the switching system in Eq. (7). Thus, we first analyze the stabilization of the switching system. Then, the state-feedback controller design method is proposed based on the genetic algorithms and some linear matrix inequalities, and the calculation steps of the controller design are listed at the end of this section.

3.1. Stabilization analysis

In order to analyze the stability of the switching system, the following two Lyapunov functions are introduced for the impulse action phase and the free motion phase respectively:

$$\begin{aligned} \text{impulse action}: \quad & V_1(\mathbf{x}) = \mathbf{x}^T(t)P_1\mathbf{x}(t), \quad t_k < t \le t_k + \tau, \\ \text{free motion}: \quad & V_2(\mathbf{x}) = \mathbf{x}^T(t)P_2\mathbf{x}(t), \quad t_k + \tau < t \le t_{k+1}, \end{aligned} \tag{8}$$

where P_1 and P_2 are symmetric positive definite matrices.

According to the Lyapunov theory, it can be seen that the asymptotic stability of the switching system can be ensured by the degression of the total virtual energy of the two subsystems. As we analyzed before, the free motion phase is an open-loop control process. Thus, the motion during this phase is uncontrollable, and the exact variation of $V_2(\mathbf{x})$ is difficult to determine. However, the degression of $V_1(\mathbf{x})$ can be certainly ensured by designing the proper state-feedback control law Eq. (6). Thus, the energy degression of the whole switching system only depends on the degression of $V_1(\mathbf{x})$ if $V_2(\mathbf{x})$ at the initial instant of each impulse period is less than its initial value of the last impulse period, which means

$$\dot{V}_2(\mathbf{x}_{t_{,+1}}) < V_2(\mathbf{x}_{t_k}). \tag{9}$$

According to the correlative analysis in [23], the stabilization of the system Eq. (7) can be ensured whether there exist two given proper positive scalars α and β such that the derivatives of $V_1(\mathbf{x})$ and $V_2(\mathbf{x})$ satisfy the following two inequalities:

$$\dot{V}_1(\mathbf{x}) < -\alpha V_1(\mathbf{x}), \quad t_k < t \le t_k + \tau, \tag{10}$$

$$\dot{V}_2(\mathbf{x}) < \beta V_2(\mathbf{x}), \quad t_k + \tau < t \le t_{k+1}. \tag{11}$$

Next, we focus on these two inequality conditions. First, based on the parameters of thruster faults, we introduce three matrices: $M_0 = \mathrm{diag}\{m_{0x}, m_{0y}\}$, $L = \mathrm{diag}\{l_x, l_y\}$ and $J = \mathrm{diag}\{j_x, j_y\}$, where $m_{0i} = (m_{li} + m_{ui})/2$, $l_i = [m_i(t) - m_{0i}]/m_{0i}$ and $j_i = (m_{ui} - m_{li})/(m_{ui} + m_{li})$ with $i = x, y$. Then, we have $M = M_0(I + L)$ and $L^TL \le J^TJ \le I$. Thus, according to Eq. (7) and the introduced matrices, the closed-loop system during the impulse action with possible thruster faults can be described as

$$\dot{\mathbf{x}}(t) = [A + \Delta A + BM_0(I + L)K]\mathbf{x}(t). \tag{12}$$

Thus, the inequality Eq. (10) can be ensured by

$$\mathrm{sym}\{P_1[A + DF(t)E + BM_0(I + L)K]\} + \alpha P_1 < 0. \tag{13}$$

By Lemmas 1 and 2 of [22], for $\kappa_1 > 0$ and $\kappa_2 > 0$, we have

$$\begin{aligned} & \mathrm{sym}\{P_1[A + DF(t)E + BM_0(I + L)K]\} \\ & \quad < \Omega + \kappa_1 P_1 DD^T P_1 + \kappa_1^{-1} E^T E + \kappa_2 P_1 BM_0 JM_0 B^T P_1 + \kappa_2^{-1} K^T JK, \end{aligned}$$

where $\Omega = \mathrm{sym}\{P_1 A + P_1 BM_0 K\}$. Then, Eq. (13) is satisfying if

$$\Omega + \kappa_1 P_1 DD^T P_1 + \kappa_1^{-1} E^T E + \kappa_2 P_1 BM_0 JM_0 B^T P_1 + \kappa_2^{-1} K^T JK + \alpha P_1 < 0. \tag{14}$$

By Schur complement, the inequality in Eq. (14) equals to

$$\begin{bmatrix} \Xi & [E^T \ \ K^T] \\ * & \mathrm{diag}\{-\kappa_1 I, -\kappa_2 J^{-1}\} \end{bmatrix} < 0, \tag{15}$$

where $\Xi = \Omega + \kappa_1 P_1 D D^T P_1 + \kappa_2 P_1 B M_0 J M_0 B^T P_1 + \alpha P_1$. Define $X_1 = P_1^{-1}$, $Y = K X_1$. Pre- and post-multiplying Eq. (15) by $\mathrm{diag}\{X_1, I, I\}$, the inequality Eq. (15) is transformed as

$$\begin{bmatrix} \Phi & [X_1 E^T \ \ Y^T] \\ * & \mathrm{diag}\{-\kappa_1 I, -\kappa_2 J^{-1}\} \end{bmatrix} < 0, \tag{16}$$

where $\Phi = \mathrm{sym}\{AX_1 + BY\} + \kappa_1 D D^T + \kappa_2 B M_0 J M_0 B^T + \alpha X_1$. Then, the inequality condition Eq. (10) is transformed into the linear matrix inequality in Eq. (16). By defining $X_2 = P_2^{-1}$ and the similarly steps, we can easily transform Eq. (11) into

$$X_2 A^T + A X_2 - \beta X_2 < 0. \tag{17}$$

Thus, we can see that, the conditions in Eqs. (10) and (11) are all transformed into linear matrix inequalities.

Next, we consider the impulse duration τ and built some connections among τ and the scalars α and β based on the condition in Eq. (9). According to Eq. (10), we also have the following result:

$$V(\mathbf{x}_{t_{k+1}}) < e^{\beta(T-\tau)} V(\mathbf{x}_{t_k+\tau}) < e^{\beta(T-\tau)} e^{-\alpha\tau} V(\mathbf{x}_{t_k}). \tag{18}$$

Thus, the condition Eq. (9) can be ensured by $e^{\beta(T-\tau)-\alpha\tau} V_2(\mathbf{x}_{t_k}) < V_2(\mathbf{x}_{t_k})$, which equals to

$$\tau > \beta T (\alpha + \beta)^{-1}. \tag{19}$$

The inequality in Eq. (19) describes the relationship between the impulse duration τ, the impulse period T and the scalars α and β.

Therefore, we can see that, the asymptotic stability of the switching system can be ensured by Eqs. (16), (17) and (19). For given impulse period T, if there exist proper scalars α, β and τ, matrices X_1, X_2 and Y, such that the conditions in Eqs. (16), (17) and (19) are satisfied, then the switching system in Eq. (7) is asymptotic stable and the desired state-feedback matrix K can be obtained by $K = YX_1^{-1}$. It can be seen that if the scalars α and β are given scalars, then the inequalities in Eqs. (16) and (17) are LMIs, which can be solved by standard software tools and the desired controller can be calculated based on the feasible solution of them. Thus, the next problem that needs to be solved is how to determine the proper scalars α, β and τ which make the LMIs (16) and (17) feasible.

3.2. Controller design algorithm

According to the analysis above, the conditions Eqs. (9)–(11) are transformed into (19), (16) and (17). Obviously, if the scalars α and β are all given scalars, then the conditions (16) and (17) are linear matrix inequalities for X_1, X_2 and Y, which can be solved by standard software tools based on the convex optimization theory. With the solution (X_1, X_2, Y), the desired feedback gain matrix K can be calculated by $K = YX_1^{-1}$. Next, an approach that combines convex optimization theory and GA is proposed.

As is well known, GA is a probabilistic search procedure based on the mechanism of natural selection and natural genetics. It has been successfully applied to different controller synthesis problems. In order to deal with our problem in this paper, an approach which combines the feasible solution of LMIs and the random search of GA is proposed. GA is used to generate the scalars α, β and τ which satisfy the inequality in Eq. (19). If Eq. (19) is feasible, then this set of scalars constitutes a solution with the corresponding feasible solution (X_1, X_2, Y) of Eqs. (16) and (17). As we discussed in Section 2, the impulse duration should be kept as short as possible, thus the minimized τ is our objective of this problem. The minimization problem can be described as

$$\min \tau \quad \mathbf{s.t}\ (19),\ (16)\ \text{and}\ (17).$$

Summarizing the above analysis, the controller design process can be generalized by the following four calculation steps based on GA and LMIs:

Step 1: Initialization. Encode the parameters α, β, τ by using the floating string as $\varphi=[\varphi_a,\varphi_b,\varphi_c]$, where $\varphi_j,(j=a,b,c)$ are three floating numbers corresponding to the scalars α, β and τ respectively. Randomly generate an initial population of N chromosomes φ_r, $r=1,2,\ldots,N$.

Step 2: Evaluate the objective and assign fitness. Check the feasibility of Eq. (19) for each set of α_r, β_r and τ_r. If (19) is infeasible, then the objective value to this group is assigned a larger value. For the sets of α_r, β_r and τ_r satisfying (19), further check the feasibility of the LMIs (16) and (17). If there exists feasible solution of the LMIs, the objective value to this group is assigned as τ_r and go to Step 3. If the LMIs are not feasible, then the objective value to this group is also assigned a larger value and go to Step 3.

Step 3: According to the assigned objective value in Step 2, choose the offspring by tournament selection approach. The group with smaller objective value has higher opportunity to be selected. In each pair of randomly selected chromosomes, the elements are probabilistically and independently swapped at each element position with a given probability (p_c) to produce pairs new chromosomes. In the population of chromosomes, the mutation operation randomly selects some elements and change them with a small probability (p_m). Elitist reinsertion guarantees that the best chromosomes in the population always survive and is retained in the next generation.

Step 4: Select a chromosome with the minimized objective value and solve the feasibility problem of LMIs. With the solution (X_1, X_2, Y), the desired state-feedback gain matrix K is calculated by $K=YX_1^{-1}$.

Remark 1. In above analysis, the impulse period T is assumed to be a given scalar. Actually, the period could be a variable scalar in practical engineering, and different impulse periods cause different transfer orbits. In this paper, we consider T as a constant scalar, which means that the interval between any two adjacent impulses is constant. For a given T, the controller can be calculated by the algorithm listed above. However, the similar algorithm can also be used to deal with the case where T is not previously given. If T is an undefined constant and its range can be generally determined, it can also be regarded as another searching objectives besides α, β and τ. Then, in calculation Step 1, the floating string φ should be defined as $\varphi=[\varphi_a,\varphi_b,\varphi_c,\varphi_d]$, where $\varphi_j,(j=a,b,c,d)$ are four floating numbers corresponding to the scalars α, β, τ and T respectively. After searching process of GA, the proper impulse period T can be found out during the given range and the state-feedback gain matrix K can also be calculated by the feasible solution (X_1, X_2, Y) of the LMIs.

4. Illustrative example

In this section, we provide three examples to illustrate the usefulness of the controller design method proposed in the above section. In Case 1, we consider a simple example where the initial relative velocity between the spacecraft is zero and the impulse period is given. In Case 2, the initial relative state becomes more complicated and the given impulse period is much longer than Case 1. In Case 3, we consider the case without given impulse period.

Case 1. Firstly, we consider a target spacecraft which is moving in a geosynchronous circular orbit with height $h=400$ km and its angular velocity is $n=1.117\times10^{-3}$ rad/s and the orbital period is 5622 s. The initial parameters of the two spacecraft are listed in Table 1.

As we analyzed in Section 2, the orbital uncertainty of the rendezvous process is given by the matrix $\Delta A=DF(t)E$. According to the structure of A, assume that

$$D=\begin{bmatrix} 0 & 0 & 0 & 0 \\ 0 & 0 & 0 & 0 \\ 0 & 0.002 & 0 & 0.004 \\ 0.002 & 0 & 0.004 & 0 \end{bmatrix},\quad E=\begin{bmatrix} 1 & 0 & 0 & 0 \\ 0 & 1 & 0 & 0 \\ 0 & 0.25 & 1 & 0 \\ -2.25 & 0 & 0 & 1 \end{bmatrix}.$$

For the possible thruster faults, assume that $m_{li}=0.8$ and $m_{ui}=1.2$ where $i=x,y$. Then, the matrices M_0 and J can be readily obtained. In this case, we consider the impulse period T is given. Assume $T=100$ s. Next, according to the calculation steps, we adopt GA to search the proper scalars α, β and τ and solve the feasibility problem of LMIs (16) and (17). The GA parameters we choose are shown in Table 2.

By the calculation of GA, the following chromosome with the minimized objective value is obtained:

$$\varphi_{\text{case1}}=[0.083303\ \ 1.7315\times10^{-7}\ \ 0.13921]. \tag{20}$$

We can see that the minimized objective $\min\tau$ is 0.13921 s. The evolution of τ in the population is shown in Fig. 1.

Table 1
Parameters of the target and chaser in Case 1.

Parameters	Values
Target orbital height	400 km
Target orbital period	5622 s
Mass of chaser	200 kg
Mean angular velocity of chaser	1.117×10^{-3} rad/s
Initial relative position	(1 km, 0.8 km)
Initial relative velocity	(0 m/s, 0 m/s)

Table 2
Parameters used by GA in Case 1.

Parameter	Population	Generations	p_c	p_m	Bounds of α	Bounds of β	Bounds of τ
Value	100	200	0.9	0.06	[0.08, 0.12]	[0, 10^{-6}]	[0, 0.5]

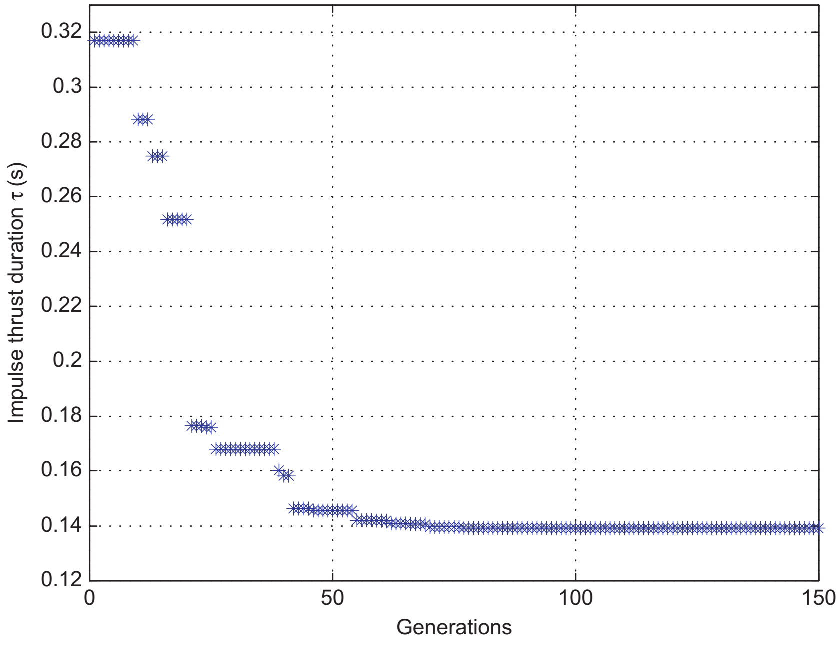

Fig. 1. Evolution of τ in the population of Case 1.

From Fig. 1, we can see that the minimized impulse duration τ can be found after nearly 70 generations. From Eq. (20), we can also obtain the proper scalars $\alpha = 0.083303$ and $\beta = 1.7315 \times 10^{-7}$, which make the LMIs (16) and (17) are feasible and the feasible solution (X_1, X_2, Y) can be readily obtained. Then, the state-feedback gain matrix K can be calculated:

$$K_{\text{case1}} = YX_1^{-1} = \begin{bmatrix} -3.8348 & -0.0228 & -67.8073 & -0.8738 \\ -0.0987 & -3.7223 & -0.8738 & -66.1275 \end{bmatrix}.$$

Thus, the state feedback controller with the form in Eq. (5) is obtained. Based on the controller, the proper impulse thrust can be calculated and generated once every 100 s.

In this case, we assume that the thruster faults occur periodically during the rendezvous process, and the percentage of the signal loss is 15% when the faults occur. Then, with the obtained state-feedback gain matrix K_{case1}, the relative position between chaser and target during the rendezvous process is shown in Fig. 2, the relative velocities along the x- and y-axes are shown in Figs. 3 and 4, respectively, and the input accelerations of chaser along the x- and y-axes are shown in Figs. 5 and 6, respectively.

From Figs. 1–6, we can see that a series of proper impulsive thrusts are generated every 100 s, and the relative position converges to zero in less than half an orbital period. Due to the longer distance along the x-axis, the needed impulse thrust along the x-axis is greater than the thrust along the y-axis. However, the convergence process along the two axes takes nearly the same time.

Case 2. Next, we consider another more complicated case. Assume that the initial velocity between two spacecraft is not zero, and the impulse period is longer than it in

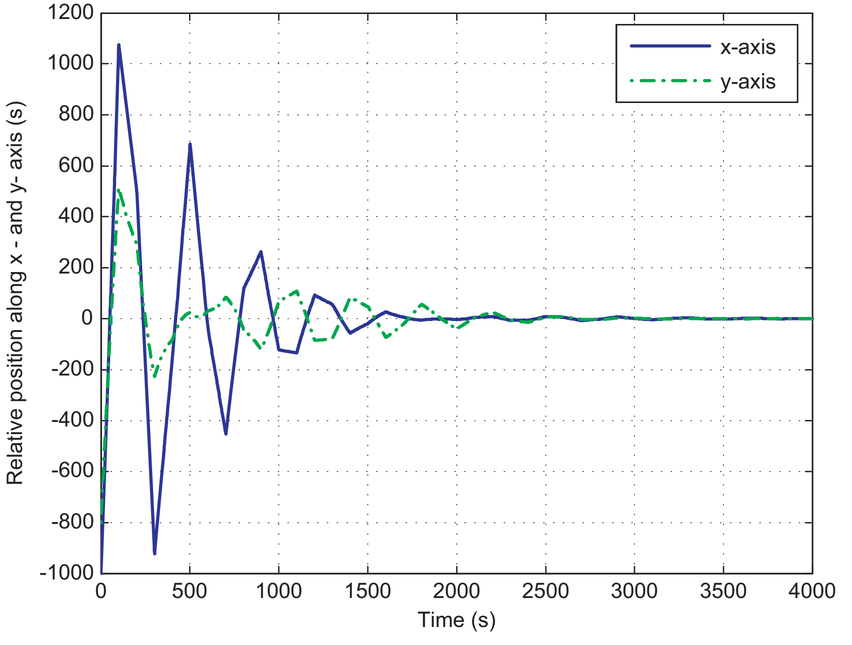

Fig. 2. Relative position along x- and y-axes between chaser and target with K_{case1}.

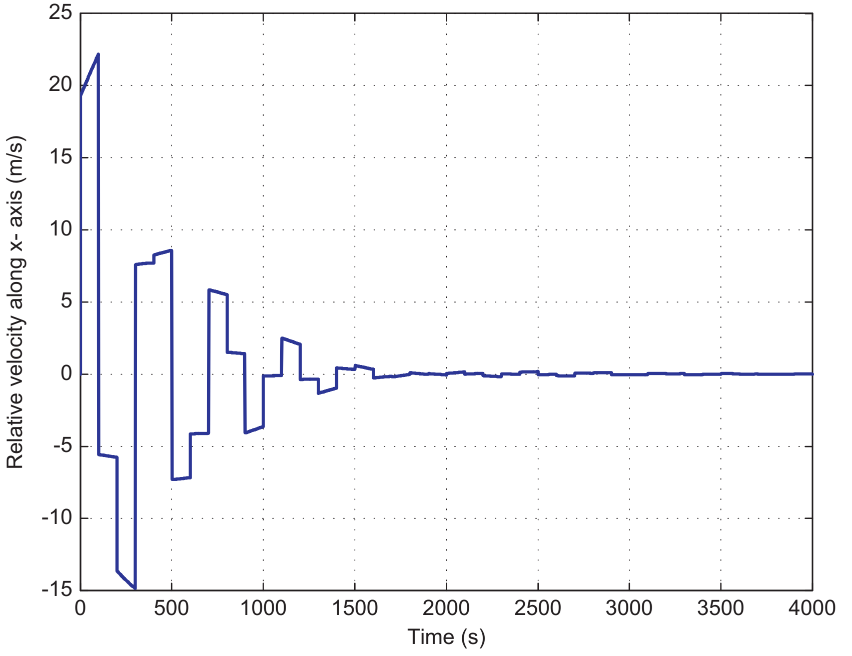

Fig. 3. Relative velocity along the x-axis with K_{case1}.

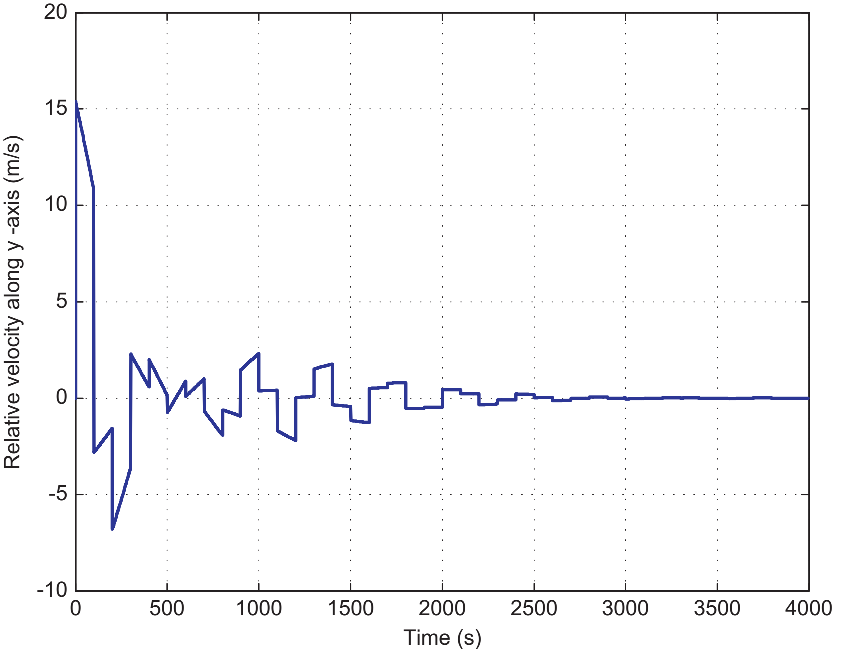

Fig. 4. Relative velocity along the y-axis with K_{case1}.

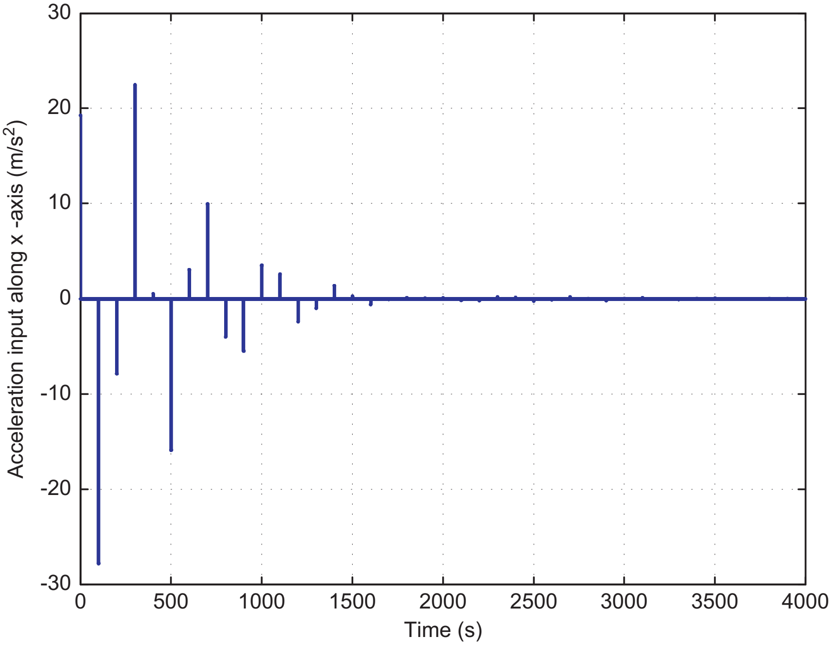

Fig. 5. Acceleration input of chaser along the x-axis with K_{case1}.

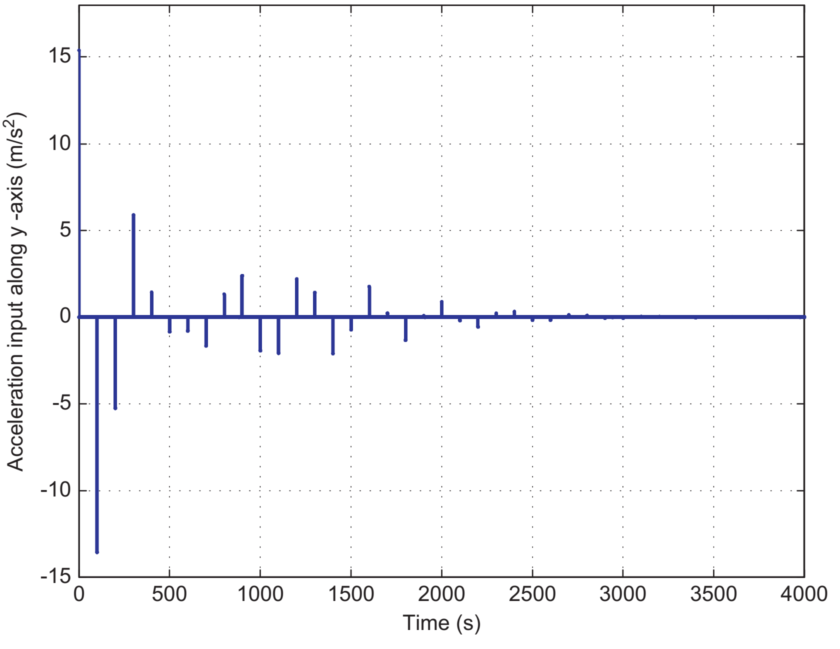

Fig. 6. Acceleration input of chaser along the y-axis with K_{case1}.

Table 3
Parameters of the target and chaser in Case 2.

Parameters	Values
Mass of the chaser	400 kg
Initial relative position	(−2 km, −1 km)
Initial relative velocity	(5 m/s, 3 m/s)
Impulse period	200 s

Case 1. The parameters that are different from Case 1 are listed in Table 3. The other parameters are same as Case 1.

Different from Case 1, the initial relative state in this case becomes $\mathbf{x}(t_0) = [-2000, 1000, 5, 3]^T$. Here, we still adopt the GA parameters which are listed in Table 2. Then, the evolution of τ in the population is shown in Fig. 7.

From Fig. 7, we can see that the minimized impulse duration τ can also be found after nearly 70–80 generations, and the obtained min τ here is longer than the min τ in Case 1. The selected chromosome with the minimized objective value is

$$\varphi_{\text{case2}} = [0.14145 \;\; 5.1851 \times 10^{-7} \;\; 0.21928].$$

By solving the feasibility problem of the LMIs, the state-feedback gain matrix K can be calculated by the set of feasible solution (X_1, X_2, Y)

$$K_{\text{case2}} = YX_1^{-1} = \begin{bmatrix} -21.3716 & -0.0867 & -226.4831 & -1.7998 \\ -0.3397 & -20.9646 & -1.7999 & -222.9688 \end{bmatrix}.$$

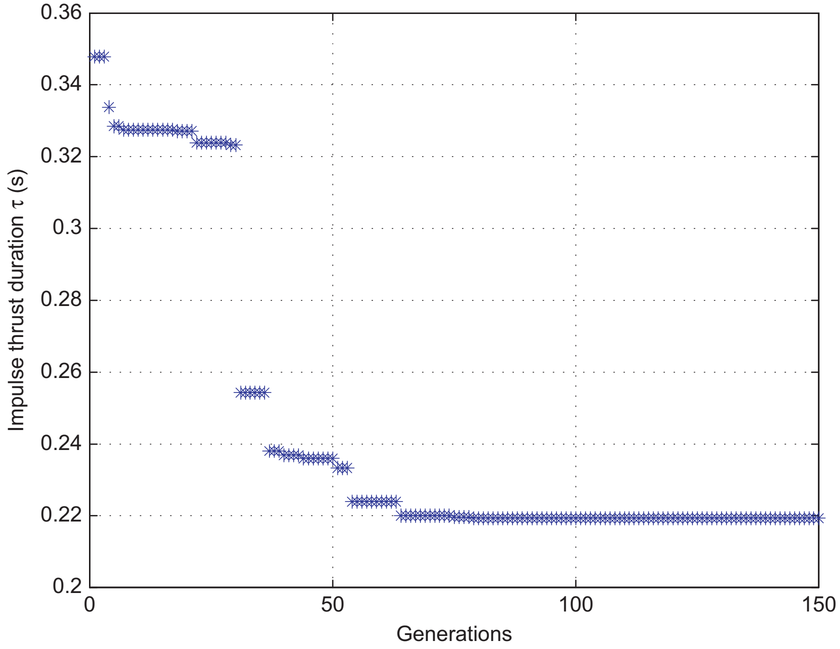

Fig. 7. Evolution of τ in the population of Case 2.

Same thruster faults pattern as Case 1 is considered here. Then, with the obtained state-feedback controller, the relative position during the rendezvous process is shown in Fig. 8. Correspondingly, we also give the relative velocity and the acceleration inputs along the x- and y-axes in Figs. 9–12 respectively.

From the figures, we can see that the rendezvous process can also be completed and the process take nearly half an orbital period, which is similar to the Case 1. However, it can also be seen that the needed impulse thrust is much greater than Case 1. This is because the initial relative position and relative velocity are all larger than Case 1. And, obviously, the longer impulse period is another important reason of the greater impulse thrust. By comparing Figs. 8 and 9 with Figs. 3 and 4, we can also find the obvious difference between these two cases. The variation of the relative velocity between the spacecraft during the rendezvous process is heavily affected by the impulse period T, which has been illustrated in Remark 1.

Case 3. Next, we consider how to determine the impulse period T due to its importance as we discussed before. As we analyzed in Remark 1, the impulse period T can also be regarded as another item of chromosome of GA. Thus, we next consider another case where T is not given. The spacecraft parameters we adopted here are same as which in Case 2, and the GA parameters are listed in Table 4. The evolution of τ in the population is shown in Fig. 13.

From Fig. 13, we can see that the minimized impulse duration τ can also be found after nearly 70–80 generations. And by the proposed algorithm, we can also obtain some sets of (α, β, τ, T) which make the LMIs feasible. The chromosome with the minimized objective value is

$$\varphi_{\text{case3}} = [0.12215 \;\; 4.5425 \times 10^{-7} \;\; 0.12012 \;\; 117.15].$$

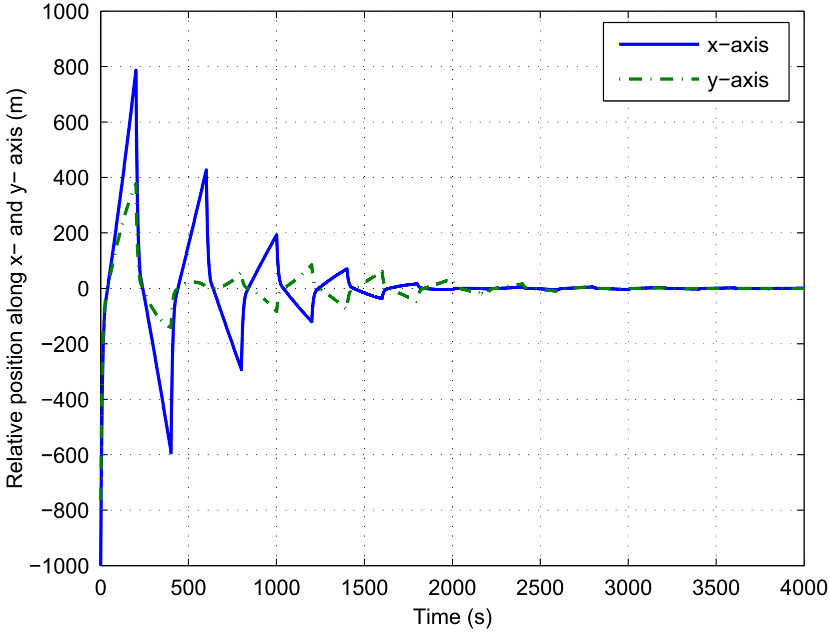

Fig. 8. Relative position along the x- and y-axes between chaser and target with K_{case2}.

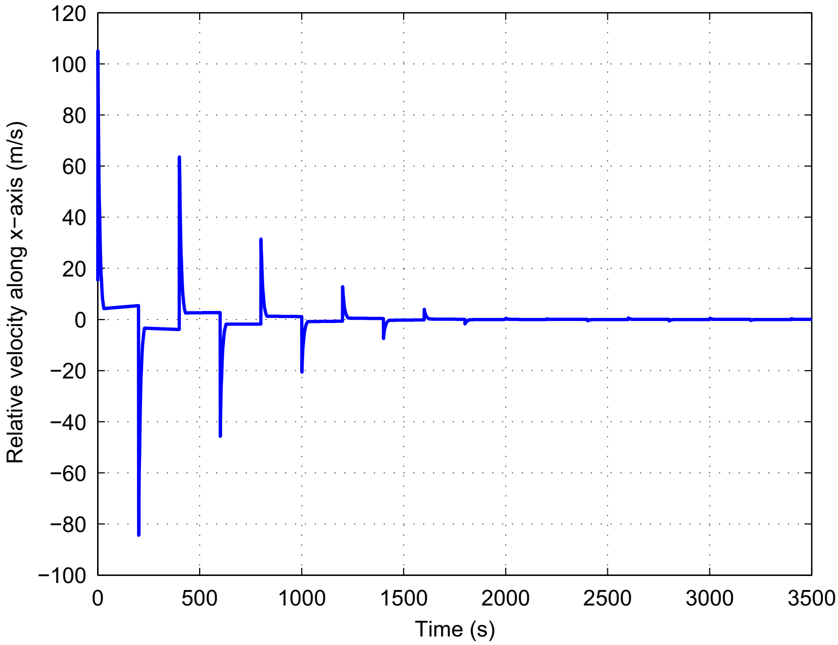

Fig. 9. Relative velocity along the x-axis with K_{case2}.

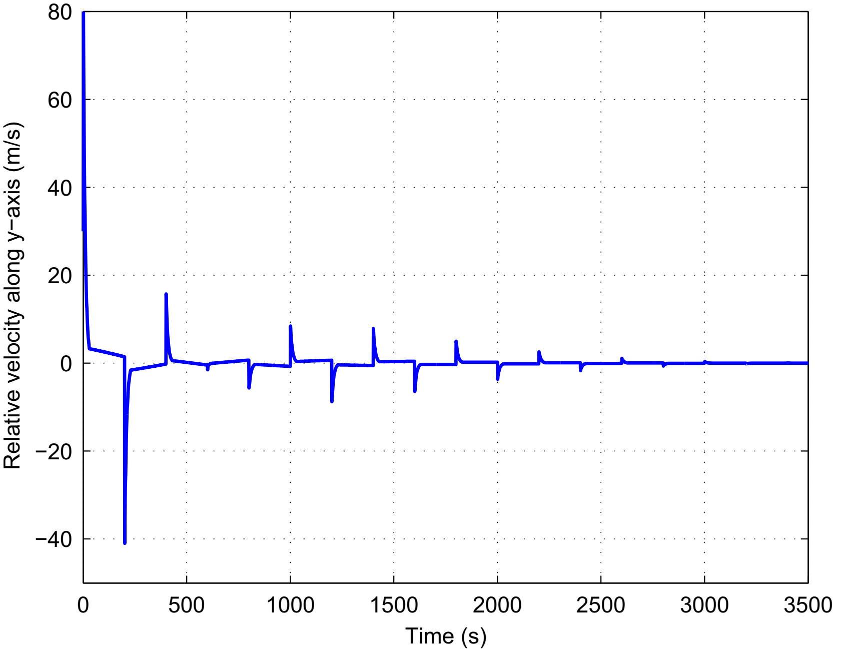

Fig. 10. Relative velocity along the y-axis with K_{case2}.

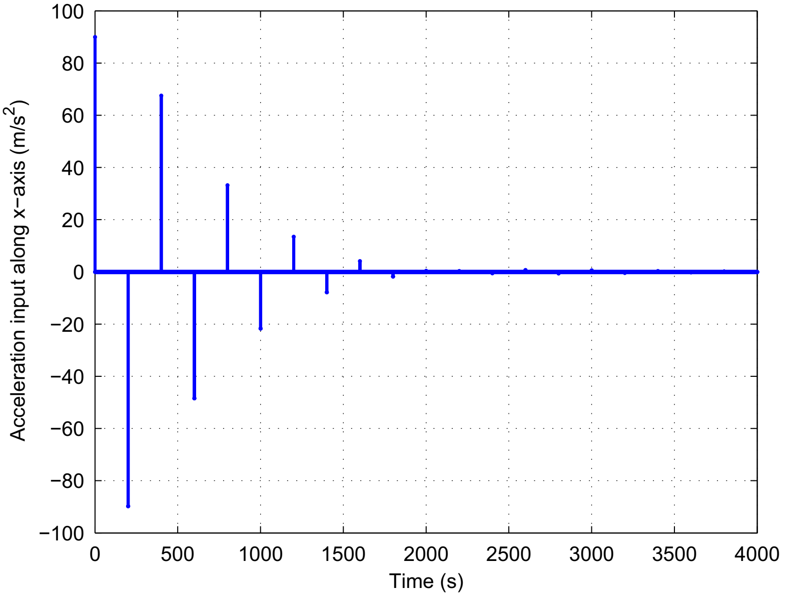

Fig. 11. Acceleration input of chaser along the x-axis with K_{case2}.

We can see that, in this case, the minimized objective min τ is 0.12012 s which is shorter than both Case 1 and Case 2, and the obtained impulse period T is 117.15 s which is between the impulse periods of Case 1 and Case 2. Obviously, the proper impulse period T

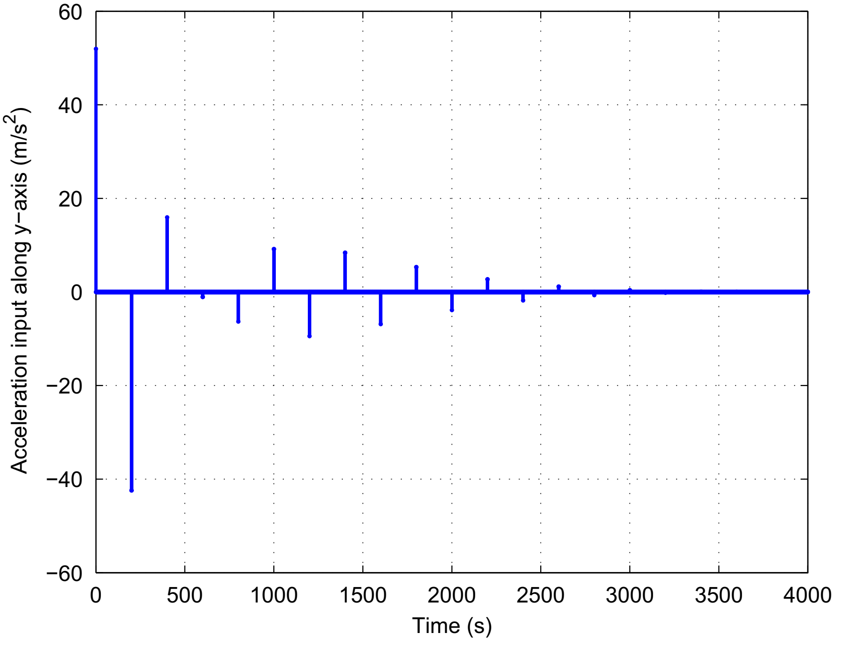

Fig. 12. Acceleration input of chaser along the y-axis with K_{case2}.

Table 4
Parameters used by GA in Case 3.

Parameter	Population	Generations	p_c	p_m
Value	100	150	0.95	0.08
Parameter	Bounds of α	Bounds of β	Bounds of τ	Bounds of T
Value	[0.05, 0.15]	[0, 10^{-6}]	[0, 1]	[100, 200]

is also determined by the proposed algorithm. Of course, there maybe exists more proper values of impulse period if we choose other region and GA parameters.

With φ_{case3}, the LMI conditions can also be solved readily according to the similar steps. By the feasible solution (X_1, X_2, Y), the state-feedback gain matrix is calculated as

$$K_{\mathrm{case3}} = YX_1^{-1} = \begin{bmatrix} -15.9555 & -0.0757 & -195.6924 & -1.8045 \\ -0.2944 & -15.6047 & -1.8045 & -192.1820 \end{bmatrix}.$$

For the limitation of the length, the simulation results of the rendezvous process with K_{case3} are omitted here.

From above cases and the analysis, we can see that the proposed algorithm is useful for the rendezvous cases whether the impulse period T is given or not. With the obtained controller, the autonomous rendezvous process can be accomplished under the orbital uncertainty and the possible impulse faults. And, it should be noted that, the designed controller is not unique. The calculation process and the results heavily depend on the parameters of the GA.

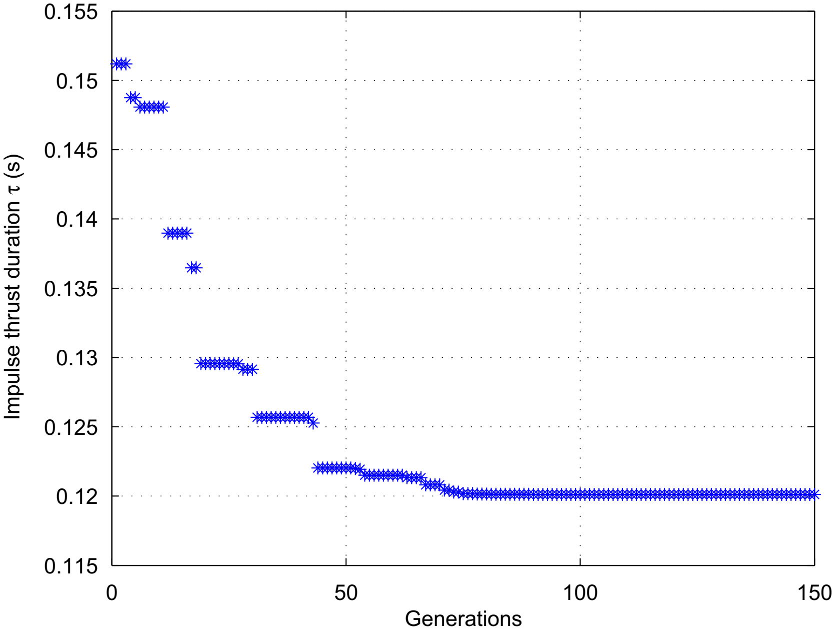

Fig. 13. Evolution of τ in the population of Case 3.

5. Conclusions

This paper studies the reliable impulsive control problem for autonomous spacecraft rendezvous. The orbital uncertainty and possible thruster faults are considered simultaneously. Based on the Lyapunov theory, the rendezvous problem is transformed into an asymptotic stabilization problem of a switching system composed of impulse action phase and free motion phase which are regarded as closed-loop system and open-loop system respectively. The proper reliable impulsive controller is obtained by solving a set of LMIs, some of whose parameters are determined by GA. With the designed controller, the needed impulse thrust is calculated according to the real-time relative state, the impulse duration is kept as short as possible, and the autonomous spacecraft rendezvous is accomplished in spit of the orbital uncertainty and the possible thruster faults. Some illustrative examples have shown the effectiveness of the proposed approach.

Acknowledgments

This work was partially supported by the National Natural Science Foundation of China (60825303, 61021002, 90916005).

References

[1] W.H. Clohessy, R.S. Wiltshire, Terminal guidance system for satellite rendezvous, Journal of Aerospace Science 27 (9) (1960) 653–658.

[2] H. Gao, P. Shi, J. Wang, Parameter-dependent robust stability of uncertain time-delay systems, Journal of Computational and Applied Mathematics 206 (1) (2007) 366–373.
[3] H. Gao, C. Wang, A delay-dependent approach to robust H_∞ filtering for uncertain discrete-time state-delayed systems, IEEE Transactions on Signal Processing 52 (6) (2004) 1631–1640.
[4] H. Gao, X. Yang, P. Shi, Multi-objective robust H_∞ control of spacecraft rendezvous, IEEE Transactions on Control System Technology 17 (4) (2009) 794–802.
[5] Y. Ichimura, A. Ichikawa, Optimal impulsive relative orbit transfer along a circular orbit, Journal of Guidance, Control, and Dynamics 31 (4) (2008) 1014–1027.
[6] D.J. Jezewski, J.D. Donaldson, An analytical approach to optimal rendezvous using Clohessy–Wiltshire equations, Journal of Astronautical Sciences 27 (3) (1979) 293–310.
[7] H. Li, B. Chen, Q. Zhou, W. Qian, Robust stability for uncertain delayed fuzzy hopfield neural networks with Markovian jumping parameters, IEEE Transactions on Systems, Man, and Cybernetics, Part B Cybernetics 39 (1) (2009) 94–102.
[8] H. Li, J. Yu, C. Hilton, H. Liu, Adaptive sliding mode control for nonlinear active suspension systems using t–s fuzzy model, IEEE Transactions on Industrial Electronics. http://dx.doi.org/10.1109/TIE.2012.2202354.
[9] Y.Z. Luo, G.J. Tang, Spacecraft optimal rendezvous controller design using simulated annealing, Aerospace Science and Technology 9 (4) (2005) 732–737.
[10] Y.Z. Luo, G.J. Tang, Y.J. Lei, Optimal multi-objective linearized impulsive rendezvous, Journal of Guidance Control and Dynamics 30 (2) (2007) 383–389.
[11] H.J. Shen, P. Tsiotras, Optimal two-impulse rendezvous using multiple-revolution Lambert solutions, Journal of Guidance Control and Dynamics 26 (1) (2003) 50–61.
[12] P. Shi, K. Boukas, On H_∞ control design for singular continuous-time delay systems with parametric uncertainties, Journal of Nonlinear Dynamics and Systems Theory 4 (1) (2004) 59–71.
[13] P. Shi, K. Boukas, R. Agarwal, Control of Markovian jump discrete-time systems with norm bounded uncertainty and unknown delay, IEEE Transactions on Automatic Control 44 (11) (1999) 2139–2144.
[14] P. Singla, K. Subbarao, J.L. Junkins, Adaptive output feedback control for spacecraft rendezvous and docking under measurement uncertainty, Journal of Guidance Control and Dynamics 29 (4) (2006) 892–902.
[15] G.L. Tang, Y.Z. Luo, H.Y. Li, Optimal robust linearized impulsive rendezvous, Aerospace Science and Technology 11 (3) (2007) 563–569.
[16] R.J. Veillette, Reliable linear-quadratic state feedback control, Automatica 31 (1) (1995) 137–143.
[17] R.J. Veillette, J.V. Medanic, W.R. Perkin, Design of reliable control systems, IEEE Transactions on Automatic Control 37 (3) (1992) 293–304.
[18] Z. Wang, F. Yang, W.C. Ho, X. Liu, Robust H_∞ control for networked systems with random packet losses, IEEE Transactions on Systems, Man, and Cybernetics—Part B 37 (4) (2007) 916–924.
[19] F. Yang, Z. Wang, W.C. Ho, M. Gani, Robust H_∞ control with missing measurements and time-delays, IEEE Transactions on Automatic Control 52 (9) (2007) 1666–1672.
[20] X. Yang, X. Cao, H. Gao, Sampled-data control for relative position holding of spacecraft rendezvous with thrust nonlinearity, IEEE Transactions on Industrial Electronics 59 (2) (2012) 1146–1153.
[21] X. Yang, H. Gao, Guaranteed cost output tracking control for autonomous homing phase of spacecraft rendezvous, Journal of Aerospace Engineering 24 (4) (2011) 478–487.
[22] X. Yang, H. Gao, Robust reliable control for autonomous spacecraft rendezvous with limited-thrust, Aerospace Science and Technology. http://dx.doi.org/10.1016/j.ast.2011.11.003, 2012.
[23] X. Yang, J. Yu, H. Gao, An impulse control approach to spacecraft autonomous rendezvous based on genetic algorithms, Neurocomputing 77 (2012) 189–196.
[24] W. Zhang, Y. Tang, J. Fang, X. Wu, Stochastic stability of genetic regulatory networks with a finite set delay characterization, CHAOS 22 (2012) 023106.
[25] Q. Zhao, J. Jiang, Reliable state feedback control system design against actuator failures, Automatica 34 (10) (1998) 1267–1272.